

Supporting Information

Tailoring the Sensitivity of Microcantilevers to Monitor the Mass of Single Adherent Living Cells

*Ilaria Incaviglia¹, Sophie Herzog¹, Gotthold Fläschner^{1,2}, Nico Strohmeyer¹, Enrico Tosoratti³, Daniel J. Müller¹ **

¹ Department of Biosystems Science and Engineering, Swiss Federal Institute of Technology Zurich (ETH), Basel, Switzerland.

² Nanosurf AG, Liestal, Switzerland.

³ Department of Mechanical and Process Engineering, Swiss Federal Institute of Technology Zurich (ETH), Zürich, Switzerland.

Experimental procedures

Cell culture. Wild-type, pKO- α V/ β 1 and pKO- α V fibroblasts⁵⁰ were provided by R. Fässler. HeLa cells (Kyoto) were provided by A. A. Hyman. All cell lines were cultured in Dulbecco's modified Eagle's (DMEM) GlutaMAX (Gibco-Life technologies) containing 100 units ml⁻¹ penicillin (Gibco-Life technologies), 100 μ g ml⁻¹ streptomycin (Gibco-Life technologies) and 10% (v/v) of fetal calf serum (FCS, Sigma). All cell lines were grown on T25 tissue culture flasks (Jet BioFil) and kept at 37°C with 5% CO₂. For the fibroblasts cell lines, tissue culture flasks were freshly coated overnight at 4°C with 50 μ g ml⁻¹ fibronectin (Calbiochem-Merck). Cells were split when reaching a confluence of 70–80% and were used for a maximum of 20 passages after thawing. Cells were regularly tested for mycoplasma contamination.

Microcantilever preparation. Tipless silicon microcantilevers (Mikromasch, HQ:NSC35/tipless/No Al) were cut using a focused ion beam (FEI Helios NanoLab 650). Standard rectangular shaped cantilevers had dimensions of approximately 120x45x2 μ m³ as previously described⁵¹. FIB-modified cantilevers present the same outer geometry; however, they had a rectangular window cut into the middle of their wider surface which was approximately 80x30x2 μ m³. Cantilevers were calibrated in air using the Sader method⁵². Before use, cantilevers were cleaned in 95% sulfuric acid for 15 min at room temperature, then rinsed in ultrapure water and dried with precision wipes (Kimtech Science). Then, cantilevers were plasma treated for \approx 15 min and subsequently incubated overnight at 4°C in PBS with the substrate of interest: 2 mg ml⁻¹ ConA (Sigma), 50 μ g ml⁻¹ fibronectin (Calbiochem-Merck) or 0.03 mg ml⁻¹ collagen type I (PureCol). For the fluorescent controls (Fig. S5), Alexa Fluor 555 NHS ester (Invitrogen) was first dissolved in DMSO at a 10 mg ml⁻¹ concentration. Then, it was added to a solution of 50 μ g ml⁻¹ fibronectin in PBS and

pure PBS in a 1:100 concentration, and incubated at room temperature for 1 h. Then, the cantilevers were coated with this solution as described above.

Picobalance setup. Single cells mass measurements were carried out using the picobalance setup as previously described⁵¹. Briefly, microcantilevers are mounted onto a customized AFM head which was equipped with piezo motors for movements in the z-axis. In addition, the AFM head presented a low-power intensity-modulated blue laser (405 nm), which served for the photo-actuation of the microcantilever *via* a current control mode. The power of the blue laser was set to 10 μW and its temperature was kept at 25°C by a laser diode controller. The infrared laser (852 nm) used to detect the deflection at the free end of the microcantilever was set to $\approx 150 \mu\text{W}$ and reflected onto a four-quadrant position-sensitive photodiode (Si PIN S5980 Hamamatsu). The picobalance was mounted on top of an inverted optical microscope (Zeiss Observer Z1) equipped with a digital camera (Hamamatsu Orca Flash 4.0) and a 10x/0.3 M27 Plan-Apochromat objective (Zeiss), which allowed for the acquisition of differential interference contrast (DIC) and fluorescent images during cell mass measurements. Finally, the picobalance had an in-house built environmental chamber which provides cell culture conditions (37°C and 5% CO₂) and prevented the medium from evaporating during cell mass measurements.

Amplitude measurements. To determine the amplitude of the two cantilever designs in air and in cell culture medium, a frequency sweep was carried out *via* a customized LabVIEW software. Each sweep is centered around the resonance frequency and acquired for a frequency range of $\pm 1.2 \text{ kHz}$ for sweeps in air and $\pm 19.5 \text{ kHz}$ for sweeps in cell medium. Each sweep was composed of 256 points acquired at 10 ms resolution. Both the sweeps in air and medium were carried out at 37°C. To convert the amplitude signal from millivolts units to nanometers, we first acquired the optical lever sensitivity for 9 cantilevers of each design

by approaching the cantilever against the bottom of a Petri dish (Ibidi, μ -Dish 35 mm, low) to get the deflection curve of the cantilever. Then, the deflection curve is fitted with a linear fit and the slope is extracted, which corresponds to the optical lever sensitivity (units mV nm^{-1}). The amplitude curves recorded in millivolts are then divided by the average value of the optical lever sensitivity to extract the amplitudes in nanometers.

Cell mass measurements. The day before measurements, cells were washed 3x in PBS previously warmed up at 37°C and serum-starved overnight in DMEM GlutaMAX containing $100 \text{ units ml}^{-1}$ penicillin and $100 \mu\text{g ml}^{-1}$ streptomycin to minimize cell cycle variations during measurements^{53, 54}. The day of measurement, a Petri dish (Ibidi, μ -Dish 35 mm, low) was mounted on the picobalance stage and filled with 1.5 ml of phenol red-free high-glucose DMEM medium, supplemented with 1 mM sodium pyruvate, 4 mM GlutaMAX, $100 \text{ units ml}^{-1}$ penicillin, $100 \mu\text{g ml}^{-1}$ streptomycin and 10% (v/v) FCS. A coated cantilever was mounted on the cantilever holder and placed inside the Petri dish with warm medium. Afterwards, the actuation and readout lasers were positioned on the cantilever and the system was let to equilibrate for 30 min. In the meantime, serum-starved cells were washed in PBS, detached using 0.25% trypsin-EDTA (Sigma) and let to recover for 15 min in the same medium which was previously added to the Petri dish⁵⁵. Afterwards, suspended cells were added to the Petri dish placed in the picobalance. The mass measurements were then performed in “continuous sweep mode” as previously described⁵⁶. First, a frequency sweep was performed to identify the resonance frequency of the bare cantilever without any cell attached. The sweep acquisition was carried out *via* a customized LabVIEW software, whereby each sweep is centered around the resonance frequency of the cantilever and acquired for a frequency range of $\pm 19.5 \text{ kHz}$. Each sweep was composed of 256 points acquired at 10 ms resolution. Then, the cantilever was brought into contact with a target cell

for 5–10 s. Usually, only cells with round contours and regular in size were chosen for measurements. Afterwards, the cantilever was retracted by 200 μm from the bottom surface of the dish, to completely detach the cell from the dish⁵⁷ and to avoid hydrodynamic effects on the cantilever movement⁵⁸. Another frequency sweep was recorded to extract the resonance frequency of the cantilever with a cell attached. Afterwards, frequency sweeps were automatically recorded every ≈ 10 s for a desired amount of time. Simultaneously, DIC microscopy images of the cell on the cantilever were acquired every 5 min and were later used for the estimation of the migration distance and the spreading area of the cell. The cell position on the cantilever was determined via an in-house software⁵⁹ using the DIC images collected during the cell mass measurements.

Cell volume measurements and expected mass calculation. A Coulter counter (Z2 Beckman Coulter Inc.) with an aperture of 100 μm was used to measure the diameter of HeLa and mouse fibroblasts cells. The counting range was set from 8 to 24 μm . The aperture was thoroughly flushed 3x with an electrolyte solution (Isoton II diluent) before minimizing the background noise. Afterwards, each measurement was performed by adding 1 ml of cell culture medium containing roughly 10^6 cells to a cuvette containing 10 ml electrolyte solution and placing it on the instrument. All cells within a volume of 0.1 ml were characterized. The cell diameter distribution obtained with the Coulter counter measurements was used to calculate the average cell volume distribution by assuming that suspended cells retain spherical shapes. The average cell volume was then used to calculate the expected mass distribution of the cells by assuming a constant density value found in literature (1.06 g ml^{-1} for HeLa cells and 1.13 g ml^{-1} for mouse fibroblast cells)⁵¹.

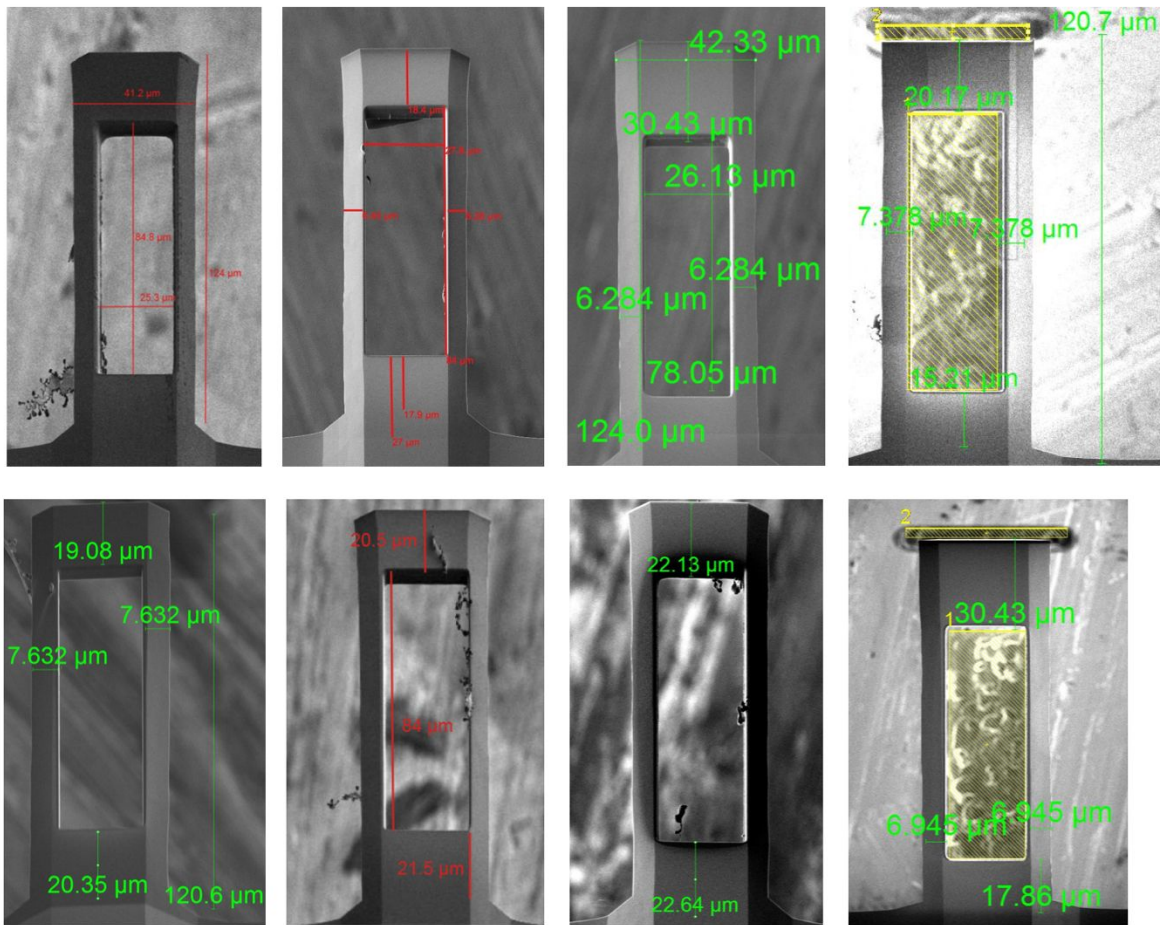
Gelatin bead fabrication and measurements. Gelatin beads were prepared as previously described⁶⁰. Briefly, gelatin (5% w/v) was dissolved in milliQ water heated to 60°C. The gelatin solution was added dropwise into a bath of liquid paraffin preheated to 60°C under constant stirring. After dropwise addition of the gelatin, the paraffin bath was emulsified 4°C for 30 minutes under constant stirring. A two times excess of 4°C cold acetone was then dropwise added to the mixture which and the solution was left to stir for an additional 30 min. The solution was then spined down at 4°C for 5 min at 2500 rpm to separate the gelatin beads from the paraffin. After removal of the supernatant, the beads were washed with 4°C acetone and spined down again. The process was repeated a total of 5 times. Gelatin beads were then resuspended in 4°C DL-glyceraldehyde aqueous solution (1% w/v) under constant stirring for 20 min. The mixture was then filtered, spined down and washed with acetone a total of five times. The beads were then kept at 4°C until used for a maximum of two weeks. On the picobalance, beads were measured following the same procedure explained for cell mass measurements.

Finite element simulations. Finite element analysis of gelatin microbeads attached to each of the two cantilever designs was performed using the solid mechanics module of COMSOL Multiphysics 5.5. The cantilevers were modelled as silicon (Young's modulus = 170 GPa), while the gelatin beads were modelled as a custom material with a Young's modulus of 12kPa and a density of 1.050 g cm⁻³ (ref.⁶¹). The cantilever together with the gelatin bead were surrounded by a 200x200x200 μm³ water cube, which is set to behave according to a Linearized Navier-Stokes Model⁶² (Fig. S6a). The cantilever motion was simulated in the solid mechanics module by selecting one end as fixed constraint and applying 1 nN boundary load in the z-direction to the opposite end. Finally, the boundary between the cantilever and the surrounding water was defined as an aeroacoustic-structure boundary in the COMSOL

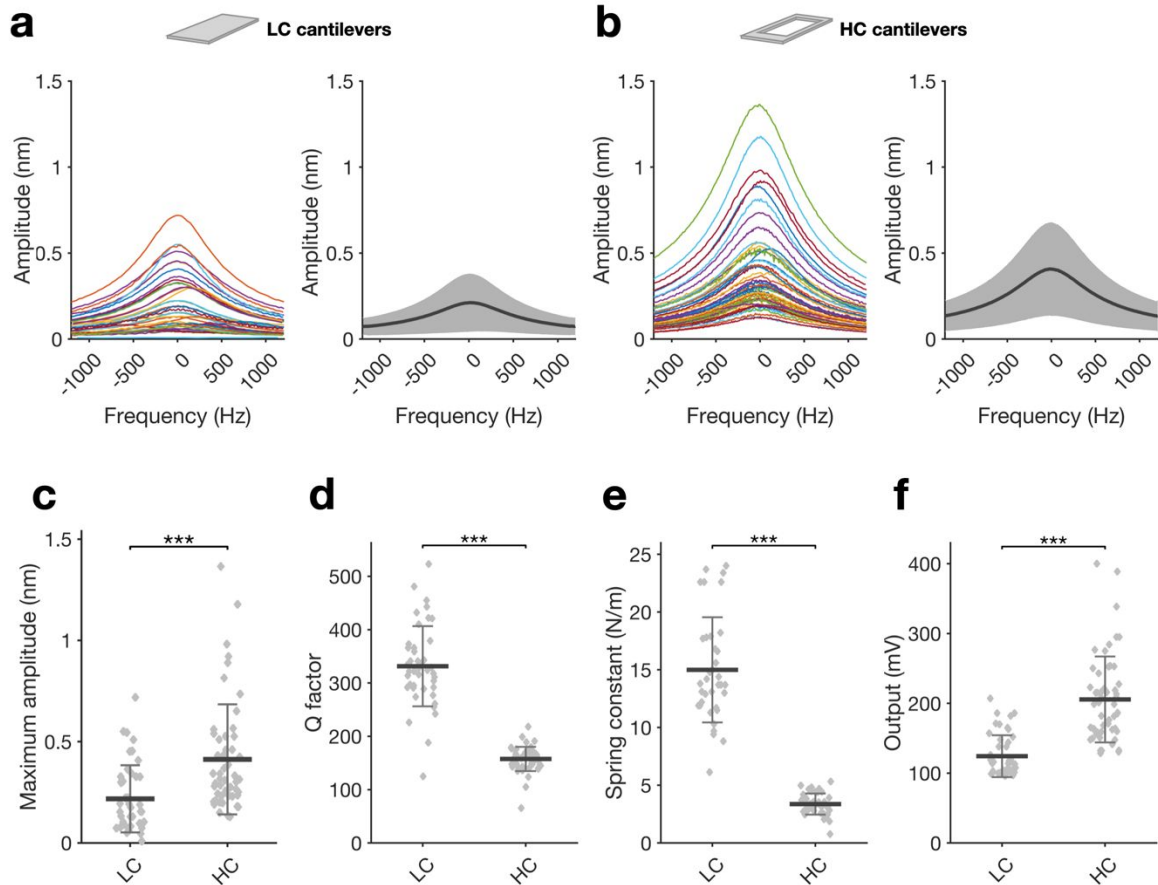
Multiphysics module. The frequency sweeps were acquired by performing a frequency domain study between 20 kHz and 80 kHz in steps of 0.5 kHz (Figure S6b).

Data analysis. For data analysis, only mitotic cells were discarded while all the other cell measurements were included. The mass and spreading area of single cells were calculated using the pyIMD software (version 0.1.3)⁵⁹. Mann–Whitney U test was used to determine significant differences between mean values. Differences were considered not significant (n.s.) if $P > 0.05$, and significance is indicated as follows: $*P \leq 0.05$, $**P \leq 0.01$, $***P \leq 0.001$. All statistical analyses were performed on Matlab R2020b.

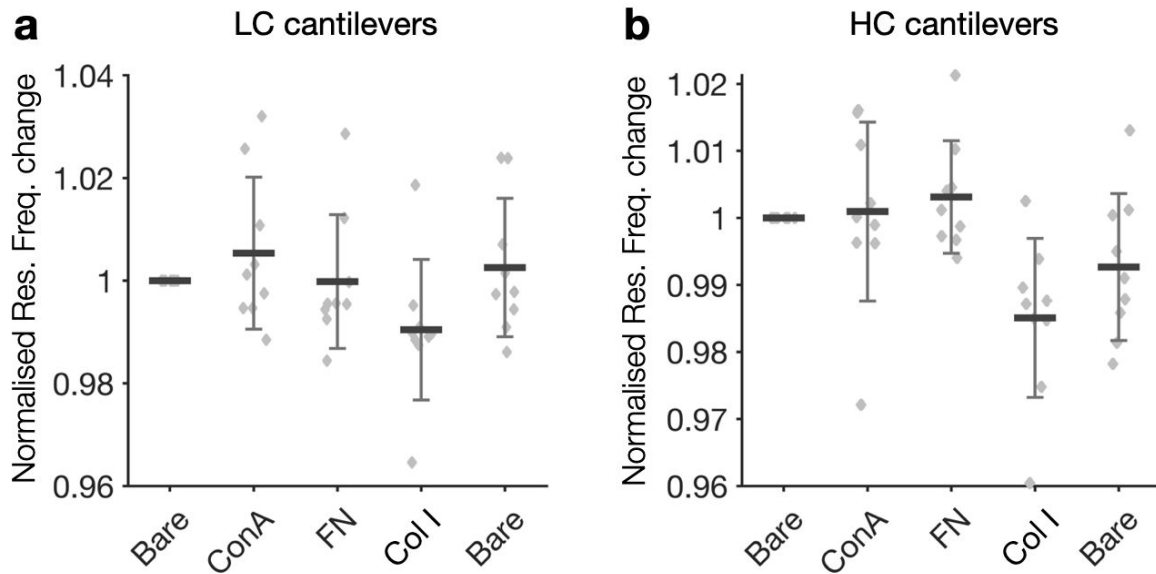
Supplementary figures



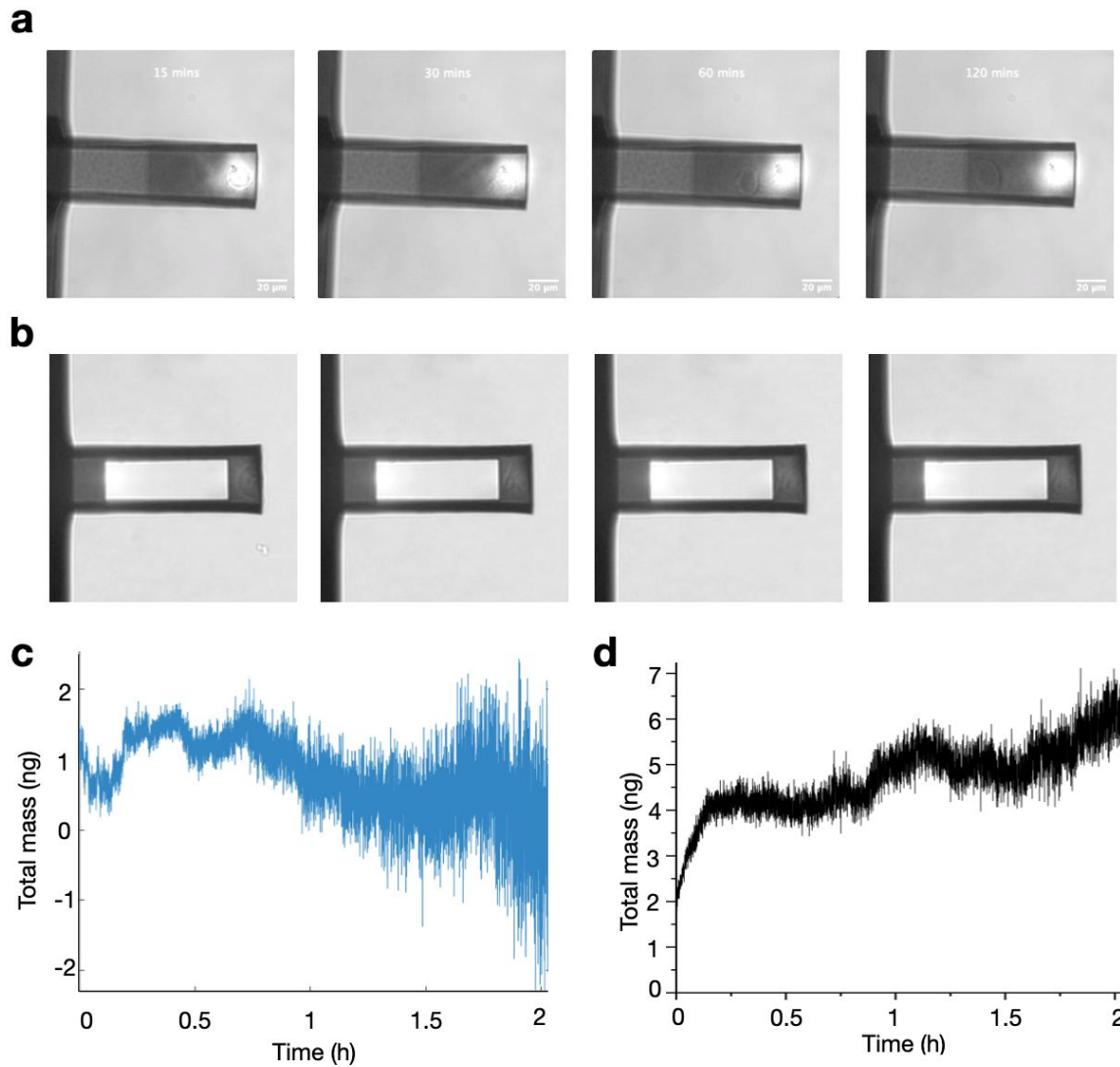
Supplementary Figure 1. Microcantilever geometry by SEM. Top view of HC cantilevers captured by SEM. The cantilever dimensions show the geometrical variations introduced by the focused ion beam (FIB) cutting process. The SEM images and all other SEM images shown in this work were acquired by D. Mathys from the Nano Imaging Lab from the Swiss Nanoscience Institute (SNI) of the University of Basel.



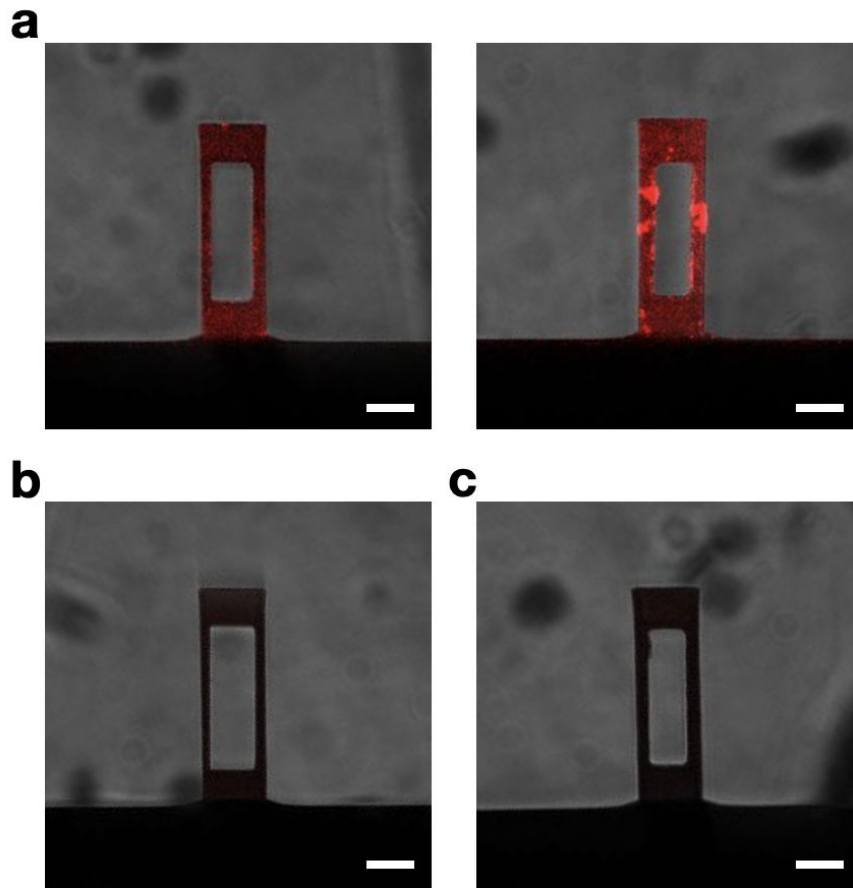
Supplementary Figure 2. Comparison of LC and HC cantilever specifications in air. **a, b**, Individual and average amplitude curves (right) for LC and HC cantilevers. Amplitudes are centered around their resonance frequency value and recorded for a frequency range of ± 1.20 kHz. Average curves are presented as mean (black line) and s.d. (grey area). **c**, Comparing the maximum amplitude between LC and HC cantilevers shows significantly higher amplitudes for HC cantilevers. **d, e**, The resonance frequency, Q factor of HC are significantly lower compared than the respective values for LC cantilevers. **f**, Reflectivity values for LC and HC cantilevers obtained for a set point of 6V. Number of independent measurements performed $n = 45$ for LC and $n = 52$ for HC cantilevers. A new cantilever was taken for each independent measurement. Statistical differences were evaluated applying the Mann–Whitney test.



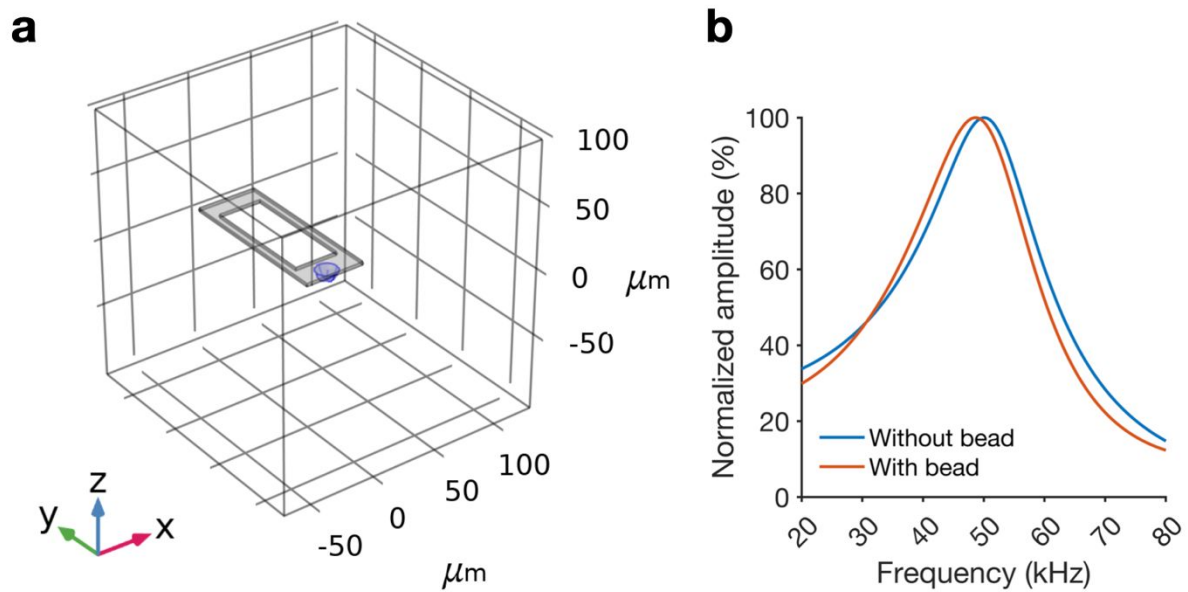
Supplementary Figure 3. Cantilever coatings do not influence its resonance frequency by more than 2%. Resonance frequency change for LC (a) and HC cantilevers (b) for different coatings measured in cell culture media at 37°C. $n = 8$ independent measurements were performed for both cantilever designs, with each measurement taking a different cantilever. Cantilevers were first cleaned in 95% sulfuric acid for 15 min at room temperature, rinsed in ultrapure water and plasma treated for ≈ 15 min as described in the Methods. Then, the cantilevers were characterized without any coating (bare) and subsequently after coating with a 2 mg ml^{-1} ConA, $50 \text{ } \mu\text{g ml}^{-1}$ fibronectin (FN) or 0.03 mg ml^{-1} collagen type I (Col I) as described in the Methods. The cantilevers were cleaned as described above after each coating step.



Supplementary Figure 4. Effect of cell migration on the correction of the cell mass measurements. **a, b**, DIC microscopy images of LC (**a**) and HC cantilevers (**b**) of a wild-type fibroblast adhering to a fibronectin-coated cantilever over the course of 2 h. Scale bar, 20 μ m. **c, d**, Recorded mass of two different cells growing on LC (**c**) and HC (**d**) cantilevers for 2 h. Since the LC cantilevers allow for larger cell migration towards the fixed end of the cantilever, the mass measurement is characterized by higher noise. All measurements were carried out in cell culture medium at 37°C.



Supplementary Figure 5. Fibronectin coating fluorescence controls. **a**, HC cantilever incubated with $50 \mu\text{g ml}^{-1}$ fibronectin labeled with Alexa Fluor 555 (described in the Methods). **b**, HC cantilever incubated with PBS mixed with Alexa Fluor 555 dye. **c**, HC cantilever incubated with PBS only. Scale bars, $20 \mu\text{m}$. All measurements were carried out in cell culture medium at 37°C .



Supplementary Figure 6. COMSOL simulations setup. a, COMSOL model of the HC cantilever (in grey, outer dimensions 120x45x2 μm^3 , cut out window 80x30x2 μm^3) with a gelatin bead (violet) attached to the free end. The gelatin bead is modeled as a hemisphere with a diameter of 8 μm . The cantilever is surrounded by a 200x200x200 μm^3 cube of water. **b,** Simulated amplitude response of bare HC cantilever without bead and with bead attached, showing the resonance frequency shift upon cell attachment.

References for Supporting Information

(50) Schiller, H. B.; Hermann, M. R.; Polleux, J.; Vignaud, T.; Zanivan, S.; Friedel, C. C.; Sun, Z.; Raducanu, A.; Gottschalk, K. E.; Thery, M.; et al. beta1- and alphav-class integrins cooperate to regulate myosin II during rigidity sensing of fibronectin-based microenvironments. *Nat Cell Biol* **2013**, *15* (6), 625-636. DOI: 10.1038/ncb2747 From NLM Medline.

(51) Martínez-Martín, D.; Fläschner, G.; Gaub, B.; Martin, S.; Newton, R.; Beerli, C.; Mercer, J.; Gerber, C.; Müller, D. J. Inertial picobalance reveals fast mass fluctuations in mammalian cells. *Nature* **2017**, *550* (7677), 500-505. DOI: 10.1038/nature24288.

(52) Sader, J. E.; Sanelli, J. A.; Adamson, B. D.; Monty, J. P.; Wei, X.; Crawford, S. A.; Friend, J. R.; Marusic, I.; Mulvaney, P.; Bieske, E. J. Spring constant calibration of atomic force microscope cantilevers of arbitrary shape. *Rev Sci Instrum* **2012**, *83* (10), 103705. DOI: 10.1063/1.4757398 From NLM Medline.

(53) Chen, M.; Huang, J.; Yang, X.; Liu, B.; Zhang, W.; Huang, L.; Deng, F.; Ma, J.; Bai, Y.; Lu, R.; et al. Serum starvation induced cell cycle synchronization facilitates human somatic cells reprogramming. *PLoS One* **2012**, *7* (4), e28203. DOI: 10.1371/journal.pone.0028203 From NLM Medline.

(54) Goranov, A. I.; Cook, M.; Ricicova, M.; Ben-Ari, G.; Gonzalez, C.; Hansen, C.; Tyers, M.; Amon, A. The rate of cell growth is governed by cell cycle stage. *Genes Dev* **2009**, *23* (12), 1408-1422. DOI: 10.1101/gad.1777309 From NLM Medline.

(55) Schubert, R.; Strohmeyer, N.; Bharadwaj, M.; Ramanathan, S. P.; Krieg, M.; Friedrichs, J.; Franz, C. M.; Muller, D. J. Assay for characterizing the recovery of vertebrate cells for adhesion measurements by single-cell force spectroscopy. *FEBS Lett* **2014**, *588* (19), 3639-3648. DOI: 10.1016/j.febslet.2014.06.012 From NLM Medline.

(56) Cuny, A. P.; Tanuj Sapra, K.; Martinez-Martin, D.; Flaschner, G.; Adams, J. D.; Martin, S.; Gerber, C.; Rudolf, F.; Muller, D. J. High-resolution mass measurements of single budding yeast reveal linear growth segments. *Nat Commun* **2022**, *13* (1), 3483. DOI: 10.1038/s41467-022-30781-y From NLM Medline.

(57) Helenius, J.; Heisenberg, C. P.; Gaub, H. E.; Muller, D. J. Single-cell force spectroscopy. *J Cell Sci* **2008**, *121* (11), 1785-1791. DOI: 10.1242/jcs.030999 From NLM Medline.

(58) Green, C. P.; Sader, J. E. Frequency response of cantilever beams immersed in viscous fluids near a solid surface with applications to the atomic force microscope. *Journal of Applied Physics* **2005**, *98* (11), 114913. DOI: 10.1063/1.2136418.

(59) Cuny, A. P.; Martínez-Martín, D.; Fläschner, G. pyIMD: Automated analysis of inertial mass measurements of single cells. *SoftwareX* **2019**, *10*. DOI: 10.1016/j.softx.2019.100303.

(60) Forni, F.; Cameroni, R.; Furioli, G.; Pifferi, G. Biodegradable microbeads for the pharmaceutical and cosmetic uses. *EP0563876A2* **1993**.

(61) Karimi, A.; Navidbakhsh, M. Material properties in unconfined compression of gelatin hydrogel for skin tissue engineering applications. *Biomed Tech (Berl)* **2014**, *59* (6), 479-486. DOI: 10.1515/bmt-2014-0028 From NLM Medline.

(62) Brunner, D.; Khawaja, H.; Moatamedi, M.; Boiger, G. CFD modelling of pressure and shear rate in torsionally vibrating structures using ANSYS CFX and COMSOL Multiphysics. *The International Journal of Multiphysics* **2018**, *12* (4), 349-358. DOI: 10.21152/1750-9548.12.4.349 (accessed 2022/08/22).